



HAL
open science

GaAs spin injector microcantilever probe assembly via a releasable 'epitaxial patch technology'

S. Arscott, Emilien Peytavit, Duong Vu, Alistair C.H. Rowe, Daniel Paget

► To cite this version:

S. Arscott, Emilien Peytavit, Duong Vu, Alistair C.H. Rowe, Daniel Paget. GaAs spin injector microcantilever probe assembly via a releasable 'epitaxial patch technology'. Proc. Eurosensors XXIV 2010, Sep 2010, Linz, Austria. pp.1039-1042, 10.1016/j.proeng.2010.09.287 . hal-02345820

HAL Id: hal-02345820

<https://hal.science/hal-02345820v1>

Submitted on 11 Jul 2022

HAL is a multi-disciplinary open access archive for the deposit and dissemination of scientific research documents, whether they are published or not. The documents may come from teaching and research institutions in France or abroad, or from public or private research centers.

L'archive ouverte pluridisciplinaire **HAL**, est destinée au dépôt et à la diffusion de documents scientifiques de niveau recherche, publiés ou non, émanant des établissements d'enseignement et de recherche français ou étrangers, des laboratoires publics ou privés.



Distributed under a Creative Commons Attribution - NonCommercial - NoDerivatives 4.0 International License

Proc. Eurosensors XXIV, September 5-8, 2010, Linz, Austria

GaAs spin injector microcantilever probe assembly via a releasable “epitaxial patch technology”

Steve Arscott^a, Emilien Peytavit^a, Duong Vu^b, Alistair C.H. Rowe^b and Daniel Paget^b

^a*IEMN, CNRS, University of Lille, Avenue Poincaré, Villeneuve d'Ascq 59652, France*

^b*PMC, CNRS, Ecole Polytechnique de Paris 91128, Palaiseau, France*

Abstract

We demonstrate that GaAs spin injector microcantilever probes can be produced using a novel releasable “epitaxial patch technology” assembly approach as apposed to a monolithic fabrication route i.e. surface/bulk micromachining. The GaAs microcantilevers are attached to fused silica support wafers; thus taking advantage of the optical and spin properties of GaAs and the mechanical properties of the silica. The microcantilever probes have been characterized for their spin injection properties and also used as atomic force microscopy (AFM) probes to evaluate their imaging capabilities. The assembly involved the production of released epitaxial semiconductor “patches” having a micrometer thickness. These patches are then assembled onto a pre-fabricated fused silica support wafer. AFM characterization revealed a resonant frequency and quality factor equal to commercial silicon-based AFM probes together with high quality images; the spin injection characterization demonstrated injected photocurrents of tens of nA and a spin polarization of ~15%.

© 2010 Published by Elsevier Ltd. Open access under [CC BY-NC-ND license](http://creativecommons.org/licenses/by-nc-nd/3.0/).

Keywords: Microsystems, MEMS, Microtechnology, Assembly, Epitaxy, Spin, Spintronics

1. Introduction

Silicon microsystems are routinely fabricated using the monolithic fabrication approach which involves the patterning (lithography and etching) of pre-deposited layers^{1,2}. However, due to materials processing incompatibility³ this approach does not necessarily lend itself well for the production of microsystems which involve a multi-materials’ approach by integrating compound semiconductors, ceramics, polymers, composite and smart materials. Hybrid microsystems built from these materials could take advantage of the various properties such materials display (mechanical, electronic, optical, magnetic...). In contrast, assembling pre-fabricated parts into microsystems could avoid materials processing incompatibilities and enable microsystems to be designed according to optimum individual material properties. Assembly using compound semiconductor “patches” has been recently demonstrated for the construction of hybrid circuits⁴ and microsystems⁵.

2. Principle

The spin polarized injector is a GaAs microcantilever fixed to a fused silica support. An assembly approach for such a device has several advantages: (i) GaAs is a direct gap semiconductor and thus has attractive optical

properties. Spin polarized photoelectrons can be optically pumped into GaAs. We take advantage of the mechanical properties of the rigid fused silica support wafer which facilitates multi-use of the probe enabling measurement repeatability. (ii) Fabrication of densely packed GaAs micrometer sized patches brings cost benefits over a monolithic MEMS approaches and no rear-side deep etching is required to release the cantilever. Optical pumping of spin polarized carriers requires that the cantilever material should be p-type in order to avoid a repulsive surface barrier, and to maximize polarization. Indeed, the spin polarization depends on the ratio of the efficiencies of spin-relaxation and of recombination. In the same way as for spin-polarized electron sources in vacuum, the best adapted strain-free source consists of highly-doped p-type GaAs ($\sim 10^{18} \text{ cm}^{-3}$) which has a typical spin polarization P of 20-30 % at room temperature for an excitation energy between 1.42 eV and 1.75 eV. Since eventual electrical injection via tunnelling occurs after diffusion across the cantilever, the thickness of the cantilever should obviously be comparable or smaller than the minority carrier charge and spin diffusion lengths.

3. Fabrication

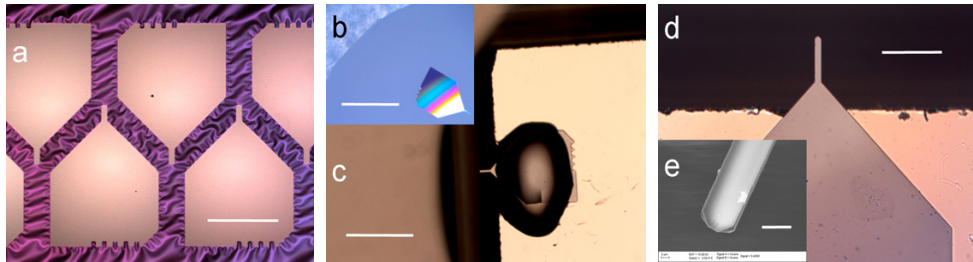


Fig. 1 Patch technology: (a) fabrication of $3 \mu\text{m}$ thick GaAs mesa "patches", scale bar = $300 \mu\text{m}$ (b) patch recuperation and storage in isopropanol, the optical microscope image shows an individual GaAs patch suspended in a water droplet, scale bar = $600 \mu\text{m}$ (c) fluidic assembling of a GaAs patch onto a pre-diced and metallized (Ti/Au/Pt/Ti/Pt) fused silica support wafer using capillary forces, scale bar = $400 \mu\text{m}$ (d) a GaAs microcantilever protruding over the edge of the fused silica support wafer (chip dimensions = $0.75 \times 2 \times 4 \text{ mm}$) following drying and ohmic contact formation ($400^\circ\text{C}/40\text{s}$), scale bar = $100 \mu\text{m}$ and (e) a scanning electron microscopy image of the tip of the GaAs microcantilever showing the crystal planes and sharp corners exposed by the wet etching ($\text{NH}_4\text{OH}/\text{H}_2\text{O}_2/\text{H}_2\text{O}$) in (a), scale bar = $10 \mu\text{m}$.

The fabrication process⁵ involves 6 main steps: (a) MBE growth of the GaInP/GaAs epitaxial layer (b) patterning of the top GaAs epitaxial layer (c) recovery of GaAs patches and storage in a liquid (d) fabrication of fused silica support layer with Ohmic metallization (e) fluidic assembly and (f) of Ohmic contact activation. First, a 100 nm thick layer of non-intentionally-doped lattice matched $\text{Ga}_{0.51}\text{In}_{0.49}\text{P}$ is grown onto a SI-GaAs (100) wafer surface ($T_g = 520^\circ\text{C}$) using gas source molecular beam epitaxy. A $3 \mu\text{m}$ thick layer of GaAs is then grown ($T_g = 580^\circ\text{C}$) onto the 100 nm thick GaInP layer at; doped uniformly with carbon; doping $\sim 1 \times 10^{18} \text{ cm}^{-3}$. Photolithography and wet etching are used to pattern $3 \mu\text{m}$ thick patches in the GaAs layer. A NH_4OH (30%)/ $\text{H}_2\text{O}_2/\text{H}_2\text{O}$ (1/1/10) anisotropic wet etch (room temperature etch rate in the [001] direction $\sim 750 \text{ nm min}^{-1}$) is used to form the GaAs patches which contain the adhesion zone and the cantilever; this wet etch is highly selective to the GaInP layer. The GaAs cantilever lateral dimensions are $10 \times 65 \mu\text{m}$ whilst the adhesion zone is $300 \times 400 \mu\text{m}$ plus a tapering to the cantilever which gives a total patch area of $\sim 0.14 \text{ mm}^2$. A photoresist (AZ1518) is then spun on to the wafer surface to protect the GaAs mesas. The wafer surface is then adhered face down to a silicon substrate using another layer of photoresist (AZ1518). The GaAs substrate is etched using an $\text{H}_2\text{SO}_4(97\%)/\text{H}_2\text{O}_2/\text{H}_2\text{O}$ (1/8/1) solution (etch rate in the [001] direction $6\text{-}10 \mu\text{m min}^{-1}$) under stirred agitation (1-5 rpm) to achieve a uniform back etch. At this point the densely packed mesa patches can be observed from underneath the 100 nm thick GaInP layer; the process causes the thin GaInP layer to buckle. The GaInP layer is then subsequently removed using a 10 second HCl (37%) etch ([001] etch rate $\sim 600 \text{ nm min}^{-1}$); this etch is selective to the GaAs mesas and leaves then embedded in the photoresist adhesion layer. The GaAs mesas are then collected into a storage bottle using a pipette. In order to fabricate the fused silica support wafers 3 inch diameter polished fused silica wafers (thickness = $500 \mu\text{m}$) were evaporated with an original "reverse sequence" Ohmic contact metallization for p-type GaAs composed of Ti/Au/Pt/Ti/Pt (20/100/10/40/10 nm), the initial Ti metallization acts as an adhesion layer to the fused silica surface and the final Pt

layer will be in contact with the GaAs patch. Next, the Pt surface is protected with a 1 μm photoresist layer (AZ1518) and a saw is used to produce the metalized rectangular fused silica support wafers having dimensions ($2 \times 4 \text{ mm} \times 750 \mu\text{m}$). In order to assemble the GaAs micro cantilevers onto the silica substrate a pipette is employed. A single patch is removed from the stock solution (isopropyl alcohol). A second pipette with a $\sim 0.2 \mu\text{L}$ drop of deionized water projecting from the end of the pipette is used to capture the GaAs patch. The droplet plus patch is then placed it onto the edge of the silica support. The resulting assembled GaAs cantilever spin injector is shown in Figure 1; it can be noticed that the anisotropic wet etch undercuts the GaAs and results in sharp edges and corners (tens of nm radius) on the cantilever, see inset to Figure 1.

4. Results and discussions

4.1 Atomic force microscopy characterization

The resonant frequency f_r of the GaAs microcantilever was measured to be 309 kHz and the quality factor Q was comparable to a commercial silicon based AFM cantilever ($f_r = 305 \text{ kHz}$, $Q > 10,000$). The GaAs cantilever (see Figure 1) is composed of a triangular portion (base = 354 μm , Length = 167) leading to a rectangular cantilever which (width = 10 μm , length = 67 μm). We calculate that the triangular part has a resonant frequency of $\sim 260 \text{ kHz}$ and the rectangular part $\sim 435 \text{ kHz}$; the measured resonant frequency was 309 kHz. Figure 2 shows atomic force microscopy images obtained in tapping mode (Bioscope, Veeco USA) using a GaAs microcantilever fabricated via the fluidic assembly route described above. Good quality images were obtained using the GaAs cantilevers. Figure 2(a) results from AFM imaging a 2 nm thick Ti mesa feature obtained using lithography and lift-off of a sputtered film and Figure 2(b) from imaging a 20 nm deep etch pit formed using a KI based wet-etch on a Au surface. As a comparison AFM images were also recorded using commercial silicon-based cantilevers which contain a nano-point at the cantilever tip (images not shown).

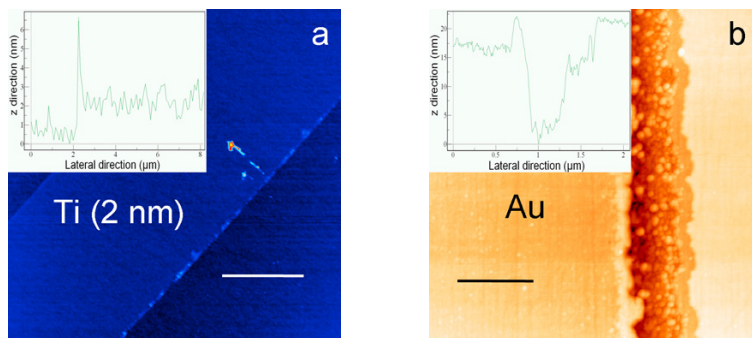


Fig. 2. Atomic force microscopy images obtained in tapping mode (Bioscope, Veeco USA) using a GaAs microcantilever fabricated via the fluidic assembly route described in Fig. 1: (a) imaging a 2 nm thick Ti mesa feature obtained using lithography and lift-off of a sputtered film, scale bar = 5 μm and (b) imaging a 20 nm deep etch pit formed using a KI based wet-etch on a Au surface, scale bar = 1 μm .

4.2 Photo-assisted tunneling

As shown in the top inset of Figure 3, tipless cantilevers excited from the rear by above bandgap light can be used for injection of photoelectrons whose spin polarization is optically controlled. The two potential difficulties of this tipless injection, related to inhomogeneities of the tunnel distance and to time instabilities of the mechanical contact, can be overcome. For each cantilever/surface distance, as controlled by *in situ* AFM-like monitoring of the deflection of the cantilever (see bottom inset of Fig. 3), 10 successive bias scans were performed. Out of contact (curve a) and close to mechanical contact (curve b), the tunnel photocurrent into a gold surface exhibits a well-defined exponential dependence whose slope decreases with decreasing distance. This shows that distance inhomogeneities do not play a significant role and that the tunnel photocurrent is dominated by the relatively

homogeneous contribution of zones of smallest distance. In contact (curve c) the bias dependence becomes nonexponential and the scans can be divided into well defined groups c_1 and c_2 with distinct correlated values of the atomic force and tunnel photocurrent at small bias. As seen from the squares, curve c_2 is a linear combination of curves c_1 and b and therefore includes some admixture of the near contact response. It is concluded that the tunnel photocurrent, in contact, is a sum of contributions from the contact zone and of a surrounding zone slightly out of contact. The source of these two responses results from the shape of the cantilever when pressed against the surface, which oscillates between two stable states as revealed by the atomic force in contact (see bottom inset, Fig. 3). It is then possible to analyze separately the current-voltage curves for the two different cases, thereby removing the effect of this bistability. Quantitative analysis is reported elsewhere⁶.

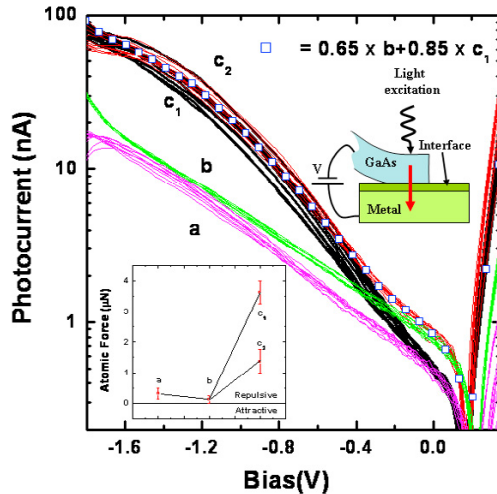


Fig. 3. Injected photocurrent bias dependences, for the geometry shown in the top inset. As verified by AFM-like in-situ (bottom inset) Curves a, b, and c, correspond to non contact, near contact, and mechanical contact configurations. Bistability of the cantilever shape give rise to distinct values of atomic force and tunnel photocurrent at low bias. (c_1 and c_2 respectively)

Acknowledgements

The authors thank J-L. Codron, C. Coinon and X. Wallart (IEMN) for the MBE growth of the samples and Dominique Deresmes for help with the AFM measurements. DV, ACHR and DP acknowledge the *Agence Nationale de la Recherche* for financial support (SPINJECT ANR-06-BLAN-0253-01)

References

- ¹Kovacs G T A, Maluf N I and Petersen K E. Bulk Micromachining of Silicon. *Proc. IEEE* 1998;**86**:1536
- ²Bustillo J M, Howe R T and Muller R S. Surface Micromachining for Microelectromechanical Systems. *Proc. IEEE* 1998;**86**:1552
- ³Spearing S M. Materials Issues in Microelectromechanical Systems. *Acta Mater* 2000;**48**:179
- ⁴Yoon J, Jo S, Chun IS, Jung I, H-S Kim, Meitl M, Menard E, Li X, Coleman JJ, Paik U and Rogers JA. GaAs photovoltaics and optoelectronics using releasable multilayer epitaxial assemblies. *Nature* 2010;**465**:329
- ⁵Arscott S, Peytavit E, Vu D, Rowe A C H and Paget D. Fluidic assembly of hybrid MEMS: a GaAs-based microcantilever spin injector *J. Micromech. Microeng* 2010;**20**:025023
- ⁶Vu D, Arscott S, Peytavit E, Ramdani R, Gil E, André Y, Bansropun S, Gérard B, Rowe A C H and Paget D. Photoassisted tunneling from free-standing GaAs thin films into metallic surfaces arXiv:1006.2915v1 <http://arxiv.org/abs/1006.2915v1> [cond-mat.mes-hall]